Conformation and Lipid Binding Properties of Four Peptides Derived from the Membrane-Binding Domain of CTP:Phosphocholine Cytidylyltransferase†

Joanne E. Johnson,‡,§ N. Madhusudhana Rao,||,⊥ Sek-Wen Hui,|| and Rosemary B. Cornell*,‡

Institute of Molecular Biology and Biochemistry and Department of Chemistry, Simon Fraser University, Burnaby, British Columbia V5A 1S6, Canada, and Membrane Biophysics Laboratory, Roswell Park Cancer Institute, Buffalo, New York 14263

Received February 11, 1998; Revised Manuscript Received April 30, 1998

ABSTRACT: We are probing the mechanism of the lipid selective membrane interactions of CTP: phosphocholine cytidylyltransferase (CT). We have proposed that the membrane binding domain of CT (domain M) consists of a continuous amphipathic α-helix between residues ∼240−295 [Dunne, S. J., et al. (1996) *Biochemistry 35*, 11975−11984]. This study examined the secondary structure and membrane binding properties of synthetic peptides derived from domain M: a 62mer peptide encompassing the entire domain (Pep62), a 33mer corresponding to the N-terminal portion (PepNH1), and two 33mers corresponding to the three C-terminal 11mer repeats, one with the wild-type sequence (Pep33Ser), and one with the three serines in the nonpolar face substituted with alanine (Pep33Ala). Peptide secondary structure was analyzed by circular dichroism, and lipid interactions were analyzed by a direct vesicle binding assay, by effects of lipid vesicles on peptide tryptophan fluorescence, and by monolayer surface pressure changes. All peptides bound to vesicles as α-helices with selectivity for anionic lipids. Binding involved intercalation of the peptide tryptophan into the hydrophobic membrane core. PepNH1, the peptide with the highest positive charge density, showed strong selectivity for anionic lipids. PepNH1 and Pep33Ser did not bind to PC vesicles; however, the more hydrophobic peptides, Pep33Ala and Pep62, did bind to PC vesicles, with apparent partition coefficients for PC that were only ∼1 order of magnitude lower than those for PC/PG (1/1). Our results suggest that the polar serines interrupting the nonpolar face of the amphipathic helix serve to lower the lipid affinity and thereby enhance selectivity for anionic lipids. Although diacylglycerol is an activator of the enzyme, none of the peptides responded differentially to PC/diacylglycerol vesicles versus pure PC vesicles, suggesting that domain M alone is not sufficient for the enzyme's response to diacylglycerol. Increases in surface pressure at an air−water interface indicated that the domain M peptides had strong surface-seeking tendencies. This supports a binding orientation for domain M parallel to the membrane surface. Binding of CT peptides to spread lipid monolayers caused surface pressure reductions, suggesting condensation of lipids in the formation of lipid−peptide complexes. At low monolayer surface pressures, Pep62 interacted equally with anionic and zwitterionic phospholipids. This suggests that one determinant of the selectivity for anionic lipids is the lipid packing density (area per molecule).

CTP:phosphocholine cytidylyltransferase (CT),[1] a key rate-determining enzyme for PC biosynthesis, is regulated by reversible membrane binding. Membrane binding and enzyme activation can be regulated by fluctuations in the membrane content of acidic lipid, and/or diacylglycerol (DAG), or by changes in the phosphorylation state of CT (*1*−*3*). Activation of the enzyme in vitro by lipid vesicles is dependent on the mole percent of acidic lipid or DAG mixed with PC (*4*−*8*). Diacylglycerol or enzyme dephosphorylation lowers the percent of acidic lipid required for activation (*3*, *9*). Both electrostatic and hydrophobic interactions mediate the membrane binding process (*7*−*10*).

Mammalian CT is organized into at least three discrete domains. The N-terminal two-thirds of the protein forms a protease-insensitive domain (*11*), which has been proposed to house the catalytic site on the basis of homologies to other cytidylyltransferases (*12*−*14*), and mutational analysis (*15*, *16*). The C-terminal region of the protein is highly phos-

† This work was supported by a grant to R.B.C. from the Medical Research Council of Canada (MT-12134) and a grant to S.-W.H. (NIH Grant GM-30969). J.E.J. was supported by a Medical Research Council Studentship.

* Corresponding author. E-mail: cornell@bohr.chem.sfu.ca. Fax: (604) 291-5583.

‡ Simon Fraser University.

§ Present address: Department of Pharmacology, University of California at San Diego, La Jolla, CA 92093-0640.

|| Roswell Park Cancer Institute.

⊥ Present address: Centre for Cellular and Molecular Biology, Uppal Road, Hyderabad 500 007, India.

[1] Abbreviations: CT, CTP:phosphocholine cytidylyltransferase; CD, circular dichroism; DAG, *sn*-1,2-diacylglycerol; PC, phosphatidylcholine; PG, dioleoylphosphatidylglycerol; DTT, dithiothreitol; BSA, bovine serum albumin; DPPC, dipalmitoylphosphatidylcholine; TFE, trifluoroethanol; Br-PC, 1-palmitoyl-2-stearoyl-9,10-dibromophosphatidylcholine; PS, phosphatidylserine; PA, phosphatidic acid; TID, 3-(trifluoromethyl)-3-(*m*-[^{125}I]iodophenyl)diazirine; LUV, large unilamellar vesicles; SUV, small unilamellar vesicle; OA, oleic acid; SM, sphingomyelin.

S0006-2960(98)00340-7 CCC: $15.00
Published on Web 06/11/1998

Peptide	Sequence	MW	Net Charge	$\langle\mu_H\rangle$	ΔG_H
Pep33-Ser	^{256}VEEKSKEFVQKVEEKSIDLIQKWEEKSREFIGS^{288}	4038	-2	0.56	-31
Pep33-Ala	^{256}VEEK**A**KEFVQKVEEK**A**IDLIQKWEEK**A**REFIGS^{288}	3990	-2	0.57	-34
PepNH1	^{236}NEKKYHLQERVDKVKKKVKDVEEKSKE**W**VQKVE^{268}	4097	+3	0.42	-22
Pep62	^{238}KKYHLQERVDKVKKKVKDVEEKSKEFVQKVEEKS IDLIQKWEE**K**SREFIGSFLEMFGPEGAL^{299}	7485	+1	0.51	-55

FIGURE 1: Amino acid sequence of the synthetic peptides. All peptides were acetylated on the N terminus and aminated on the C terminus. Underlined residues correspond to residues changed from the original sequence. $\langle\mu_H\rangle$ = the average helical hydrophobic moment (*58*, *59*), generated using the program PepPlot (Genetics Computer Group, Madison, WI). ΔG_H = the sum of transfer free energies in kilocalories per mole for all the residues in the hydrophobic faces (shaded residues and serine in Figure 2), using the GES algorithm (*50*).

phorylated in vivo (*17*−*19*). Membrane binding in vivo is accompanied by dephosphorylation of the enzyme (*1*, *20*). The degree of phosphorylation modulates the enzyme's membrane affinity (*2*, *3*, *19*).

Portions of the ~60-residue region linking the catalytic and phosphorylation domain (domain M) form an amphipathic helix in the presence of lipid bilayers or amphiphiles such as SDS (*10*, *21*). This type of structure mediates the lipid binding of several other proteins, including apolipoproteins (*22*−*24*), prostaglandin H2 synthase-1 (*25*), factor VIII (*26*), oleosin (*27*), various lytic peptides (*28*), and perhaps ADP ribosylation factor (ARF; *29*). Abundant evidence supports a membrane-binding role for domain M. Removal of this domain by proteolysis (*11*) or mutation (*16*, *18*, *19*) resulted in a loss of membrane association in vitro or in vivo. Domain M is selectively labeled by hydrophobic photoreactive probes (*30*).

We have previously studied a 33mer peptide corresponding to residues 256−288 of CT, the C-terminal portion of domain M containing a series of three tandem 11mer repeats (*10*). A helical structure and membrane intercalation of the peptide were promoted by anionic lipid but not by zwitterionic lipid vesicles or vesicles containing DAG, as determined by circular dichroism and peptide tryptophan fluorescence. The results of this study suggested a membrane-binding role for this portion of domain M, in which anionic membranes selectively stabilize a helical structure, which becomes embedded in the membrane.

In this study, we have analyzed three new synthetic peptides derived from domain M. To determine if the entire domain M region can form an amphipathic helix in the presence of membrane bilayers, and to explore whether the N-terminal portion of domain M confers sensitivity to DAG, we have studied a peptide corresponding to the 33 N-terminal residues of domain M and a 62-residue peptide corresponding to the entire region (Figure 1). The 11mer repeat motif of domain M contains three serines which interrupt the hydrophobic face of the amphipathic helix. To examine the functional role of these serines, a third peptide was generated in which the serines were triply substituted with alanine. We compared the binding of these peptides to lipid vesicles of various compositions. The influence of these vesicles on the peptides' secondary structure was monitored by CD, and the polarity of the peptides' tryptophan environment was assessed by fluorescence spectral shifts.

Since domain M is flanked on either side by domains that are accessible to proteases (*11*), it is envisioned that this domain, and peptides derived from it, would bind only to the outer monolayer of a membrane, with helix axes parallel to the bilayer surface. However, no data explicitly exclude the possibility that the peptides could bind as helical bundles in a transbilayer arrangement. Thus, we investigated the ability of peptides from domain M to bind to monolayer lipid films. Variation of the initial monolayer surface pressure was exploited to examine the role of lipid packing pressure on the peptides' binding selectivity.

Our results support a model whereby the entire domain M can form a surface-oriented amphipathic α-helix, with selectivity for anionic membranes.

EXPERIMENTAL PROCEDURES

Materials. Egg PC, dioleoyl-PG, and 1-palmitoyl-2-stearoyl-9,10-dibromo-PC were purchased from Avanti Polar Lipids (Alabaster, AL). Oleic acid and *o*-phthaldialdehyde were from Sigma. *sn*-1,2-Diacylglycerol was generated by phospholipase C digestion of egg PC as described (*31*). Microcon-100 filtration units were purchased from Amicon (Beverly, MA). Lipids were stored in $CHCl_3$ stocks at −20 °C under nitrogen. The concentration of these stocks was checked periodically by measuring phospholipid phosphorus (*32*). The purity of the stocks was checked by thin layer chromatography as described (*10*).

Peptide Synthesis. Peptides corresponding in sequence to different portions of the amphipathic helix region of CT (*33*) were synthesized and HPLC purified by I. Clark-Lewis and P. Owen (University of British Columbia, Vancouver, BC) as described (*34*). The sequences and calculated molecular weights corresponding to each peptide are shown in Figure 1. The peptides were acetylated on the N terminus and aminated on the C terminus to eliminate the influence of the charged terminal groups. The peptides were stored as solids at −80 °C. Stock solutions of the peptides were made in TE buffer [10 mM Tris-HCl (pH 7.4) and 1 mM EDTA] or HEPES buffer [10 mM HEPES (pH 7.4)] as described previously (*10*).

Gel Filtration Analysis of Peptide Aggregation State. A Sephadex G50 column (1 cm × 30 cm) was equilibrated and eluted with TE buffer at a flow rate of 0.4 mL/min. Peptide samples (~25 nmol) were dissolved in 200 μL of TE buffer containing 10% glycerol. Protein elution was monitored by UV absorbance at 280 nm. A molecular weight scale for the column was calibrated with cytochrome

c (12 400), aprotinin (6500), insulin (5700), and insulin treated with 50 mM DTT at 37 °C for 2 h so it would dissociate into β (3500)- and α (2200)-subunits. V_o and V_t for the column were determined using BSA (67 000) and bromphenol blue (700), respectively.

Preparation of Lipid Vesicles. Vesicles were prepared by hydration of dried lipid in TE buffer, followed by probe sonication for at least 20 min or until the solution clarified. Titanium debris was removed by centrifugation at 20000*g* for 5 min. All vesicles were used on the day of preparation. For the vesicle−peptide binding assay, some vesicles were spiked with trace amounts of [Me-^{3}H]DPPC, added to solvent-mixed lipids to monitor lipid recovery.

Peptide−Vesicle Binding Assay. Peptide stocks and lipid vesicles used in this assay were made in 10 mM HEPES (pH 7.4). Peptide (12 nmol) and varying amounts of lipid vesicles between 0 and 3600 nmol were incubated at room temperature for 10 min in a total volume of 200 or 300 μL of 10 mM HEPES (pH 7.4). Samples were then transferred to a Microcon-100 filtration unit (molecular weight cutoff of 100 000) and centrifuged at 3000*g* for 4−7 min, until all but 5−10 μL had gone through the filter. The filter was rinsed with 100 μL of HEPES buffer and centrifuged again for 2−3 min. Lipid vesicles and bound peptide were recovered from the filter by rinsing with 100 μL of HEPES (pH 7.4), 0.1 M NaCl, and 0.15 mM Triton X-100. Unbound peptide was in the flow-through fraction. Peptide in both fractions was quantified with an *o*-phthaldialdehyde assay (see below). Apparent partition coefficients (Table 1) were calculated using the equation K_x = (moles of bound peptide/moles of accessible lipid)/(moles of free peptide/moles of H_2O). $K_x = K_p \times 55.5$ M, where K_p is the molar partition constant (*35*). Accessible lipid (outer leaflet) was estimated as 0.5(total lipid) for PC vesicles and 0.6(total lipid) for anionic lipid vesicles. Calculations used values in which binding was >20 and <90%, i.e., near the middle of the binding curves, and were carried out only for samples in which peptide recovery was >85%.

o-Phthaldialdehyde Assay for Peptide Quantitation (36). Peptide samples were in HEPES (pH 7.4) since Tris contains an interfering primary amine. Standard curves composed of 0−6 nmol of the peptide to be assayed were analyzed with each experiment. To a 100 μL sample of peptide were added 0.5 mL of 0.05 M sodium borate (pH 10) and 0.5 mL of 0.5% (v/v) β-mercaptoethanol in ethanol, vortexing well after each addition. *o*-Phthaldialdehyde (10 mg/mL in methanol) was diluted 10-fold in 0.05 M borate (pH 10), and 0.5 mL of this solution was added to the peptide assay solution while it was vortexed. The samples were incubated at room temperature for exactly 20 min before measurement on a Perkin-Elmer MPF-44B fluorescence spectrophotometer, as the fluorescence intensity decayed slightly over time. The fluorescence intensity (excitation at 340 nm, emission at 440 nm) was proportional to the peptide concentration over the range used. The presence of lipids in excess of 500 nmol interfered with the fluorescence analysis; this amount of lipid was present only in some of the retentate fractions of binding reactions with PC.

Circular Dichroism. Samples contained 25 or 30 μM peptide and/or sonicated lipid vesicles. Background samples were composed of lipid vesicle suspensions lacking peptide. Samples were incubated for >5 min at room temperature before analysis. Measurements were taken on a Jasco 700 spectropolarimeter using the conditions described previously (*10*). Spectra were smoothed and corrected for background lipid absorbance. Values are expressed as mean residue molar ellipticity [θ]. The percent helix was estimated as described previously (*10*, *37*−*39*).

Fluorescence Studies. The samples in TE buffer contained 3.25 μM peptide and 0.5 mM lipid vesicles (or 0.162 mM lipid in the case of Pep62). For iodide quenching experiments, samples in TE buffer contained peptide, lipid, 10 mM $Na_2S_2O_3$, and the indicated concentration of NaI added from a 4 M stock. NaCl, which does not quench fluorescence, was added to maintain a constant ionic strength of 0.2 M. For quenching by brominated lipid, 9,10-dibromo-PC was solvent mixed at 50 mol % with the other lipid components. Lipid and peptide were preincubated at room temperature for >5 min prior to recording spectra. The excitation wavelength was 280 nm, and the emission spectra (300−420 nm) were recorded at 21 °C on a Perkin-Elmer MPF-44B or SLM 4800C fluorescence spectrophotometer with excitation and emission slits of 8 and 4 nm, respectively. The spectra were corrected for fluorescence due to the lipid alone.

Surface Pressure Measurements. Surface pressure was measured at room temperature using a Wilhelmy plate and a Cahn RG electric balance (*40*). Lipid dissolved in $CHCl_3$ was spread on a custom-made circular trough (d = 4.5 cm; total volume of 12.5 mL). The subphase, 10 mM HEPES (pH 7.4), was circulated with a peristaltic pump. The circulation rate was adjusted so that minimal and reproducible pressure changes occurred over several hours of observation. These background pressure changes were subtracted from the surface pressures measured in the presence of lipids and/or peptides. The lipid was spread at various surface pressures and was equilibrated before injection of the peptide into the subphase. Pressure changes were recorded after 30 min and were accurate within ±1 dyn/cm. Standard surface active compounds were used to calibrate the instrument.

RESULTS

Properties of the Peptides. The sequences of four peptides corresponding to the putative membrane binding region of CT are shown in Figure 1. Helical wheel projections illustrate the highly amphipathic character of each peptide, with a highly charged polar face and a 110−120° nonpolar sector (Figure 2). Each sequence contains a tryptophan residue within the nonpolar face. The fluorescence of this tryptophan could be monitored to assess changes in the environment of the peptide. (1) Pep33Ser corresponds to residues 256−288 in rat liver CT, the C-terminal sequence of domain M. This peptide was originally studied by Johnson and Cornell (*10*). It consists of three 11-residue repeats. The peptide, with a net charge of −2, contains nine negatively charged and seven positively charged residues. There are three serine residues in register which interrupt the otherwise hydrophobic face of the helix. (2) Pep33Ala corresponds to the same sequence as Pep33, except the three serine residues on the hydrophobic face (Ser260, -271, and -282) are changed to alanine, thereby increasing the number of hydrophobic residues on the nonpolar helical face from 10 to 13. (3) PepNH1 corresponds to the 33 N-terminal residues of domain M (residues 236−268). This peptide,

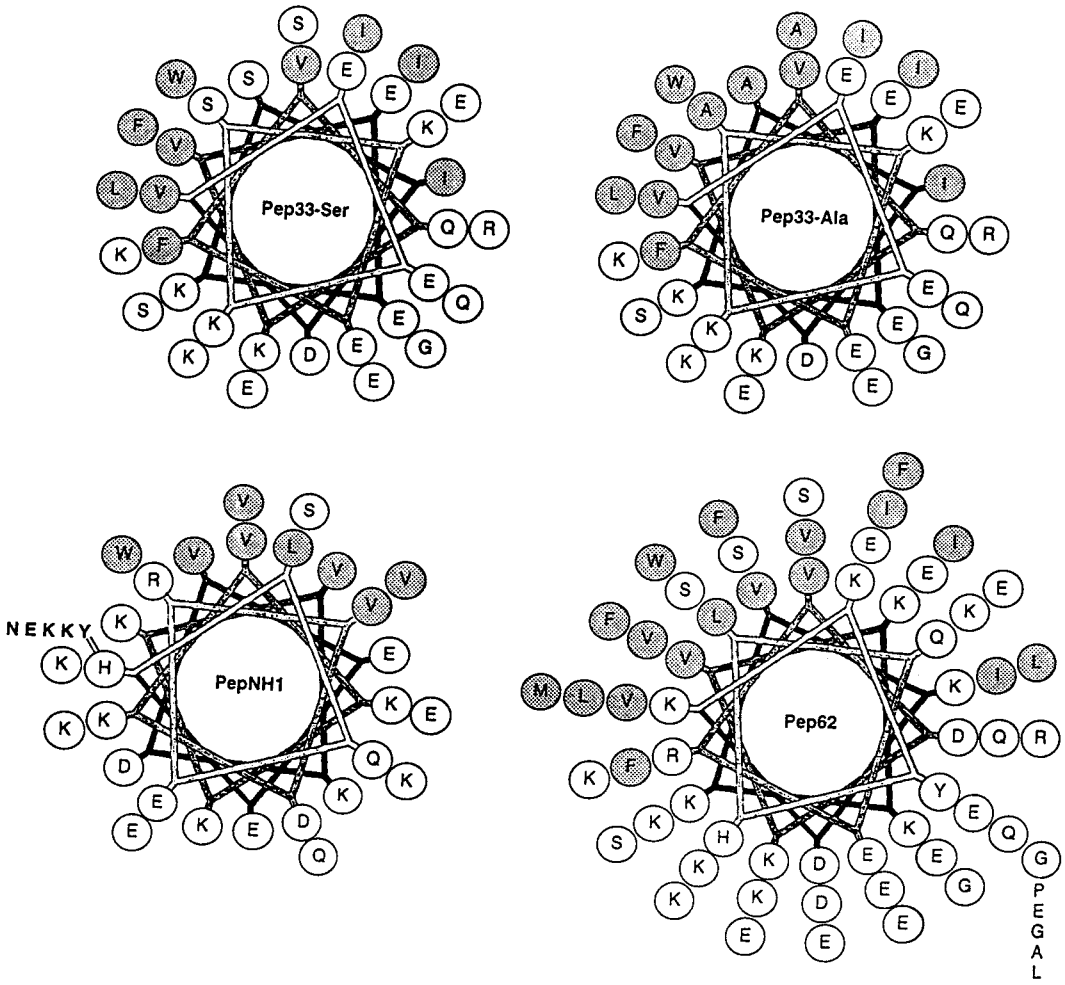

FIGURE 2: Helical wheel projections of the peptides. Hydrophobic residues are shaded, demonstrating the amphipathic nature of the helix. Only the helical portions of PepNH1 and Pep62 deduced from two-dimensional NMR solution structures are displayed (see ref *21*).

with a net charge of +3, has eight negatively charged and eleven positively charged residues, as well as a histidine residue. Since this region contained no tryptophan residues, a Trp residue was substituted for Phe at residue 263. Similar substitutions have been implemented in studies of other peptides, with no change in properties (*41*, *42*). PepNH1 contains only eight nonpolar side chains. (4) Pep62 corresponds to the entire domain M of CT (residues 238−299), which constitutes a discrete exon in the mouse CT gene (*43*). This peptide, with a net charge of +1, contains 14 negatively charged and 15 positively charged residues, as well as one histidine residue. Pep62 contains 18 nonpolar side chains.

In dilute buffer, the majority of each 33-residue peptide (Pep33Ser, PepNH1, and Pep33Ala) eluted from a Sephadex G-50 gel filtration column with an apparent molecular weight of approximately 8000, demonstrating that the peptides are not associated in large aggregates (data not shown). The molecular weight of each 33mer peptide monomer is ∼4000. Thus, each peptide eluted with an apparent molecular weight of a dimer. Approximately 5−10% of the Pep33Ala eluted as a large aggregate (>66000) in the void volume of the column. Pep62 was not analyzed by gel filtration. Crosslinking of Pep62 with excess gluteraldehyde in dilute buffer and analysis of the apparent molecular weights of the crosslinked species by SDS−PAGE revealed a mixture of monomer, dimer, trimer, and higher oligomers in the proportion 50/10/4/3 (data not shown).

Direct Peptide−Vesicle Binding Measurements. Binding to PC/oleic acid (1/1), PC/PG (anionic), and PC (nonanionic) vesicles was analyzed by an assay in which free peptide was separated from vesicle-bound peptide by filtration in a Microcon-100 filtration unit (*10*). Recoveries of PepNH1, Pep33Ser, and Pep33Ala in the filtration assay were >85%. The recovery of Pep62 in the presence of lipid was >85%; however, its recovery in the flow-through fraction was poor in the absence of lipid, and the balance was not recovered on the filter. We assume that some of this peptide absorbed onto the Microcon unit.

The binding of the four peptides to PC and PC/oleic acid vesicles is shown in Figure 3. With increasing concentrations of anionic lipid, the amount of each peptide recovered in the flow-through fraction decreased, while the amount retained on the filters increased.

Only Pep62 and Pep33Ala bound to PC vesicles. Over the range of lipid/peptide ratios tested, binding of PepNH1 or Pep33Ser to PC vesicles was not detected (Figure 3A). This indicates that electrostatic interactions are more important for these peptides than for Pep62 or Pep33Ala. The latter have larger hydrophobic faces. That Pep33Ala bound to PC vesicles, whereas Pep33Ser did not, indicates that increasing the hydrophobicity of the nonpolar face of the amphipathic helix reduces the stringent specificity for anionic lipid.

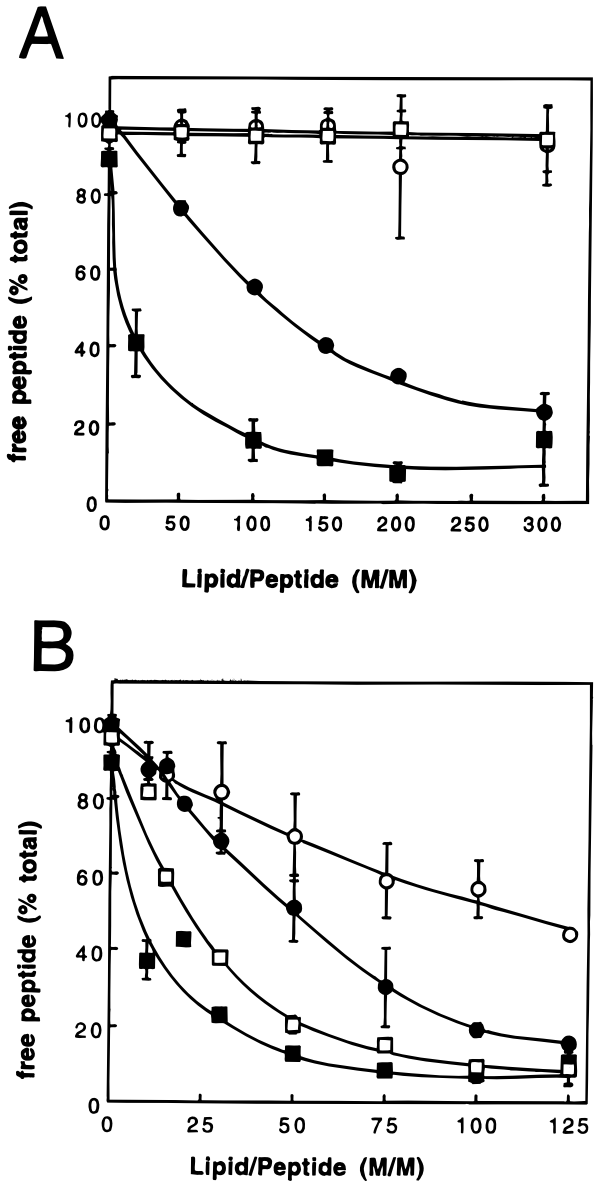

FIGURE 3: Binding of peptides to vesicles as a function of the amount of lipid. Peptide (12 nmol) was incubated with the indicated amount of PC (A) or PC/oleic acid (1/1) (B). The unbound peptide was separated from the vesicles by filtration and quantified as described in Experimental Procedures: Pep33Ser (○), Pep33Ala (●), PepNH1 (□), and Pep62 (■). Note different *x*-axis scales are used in panels A and B.

The apparent molar partition coefficient values of the peptides for PC, PC/oleic acid, and PC/PG are given in Table 1. All peptides demonstrated higher affinities for PC vesicles containing anionic lipid than for PC alone. The largest peptide, Pep62, bound to PC/oleic acid or PC/PG vesicles with the highest affinity. Of the 33mer peptides, PepNH1 had the highest affinity for anionic membranes. This peptide is also the sole 33mer peptide with a net positive charge (+3, Figure 1). Pep33Ala had a higher affinity for anionic and nonanionic vesicles than did Pep33Ser, demonstrating that substituting the serine residues located on the nonpolar helical face with alanine increases the lipid affinity (Figure 3 and Table 1).

Association of the Peptides with Lipids Is Accompanied by a Change in Secondary Structure to a Helical Conformation. CD spectra were acquired to determine the preferred secondary structure of the peptides. The CD spectrum of each peptide in TE buffer alone was indicative of a predominantly random structure with only a small amount of helix, 12−14% (Figure 4 and Table 2). Trifluoroethanol (TFE) promotes favored secondary structure in peptides and proteins by promoting intramolecular hydrogen bonding (*39*). TFE (50%) changed the spectrum of each peptide to one indicative of an α-helical structure, with the characteristic minima at 208 and 222 nm (Figure 4). The helical content of the peptides in TFE was approximately 50% (Table 2). Thus, CD experiments demonstrated a propensity for the entire domain M and its constituent parts to form helical structures, consistent with secondary structural predictions (*33*).

Table 1: Peptide−Lipid Partition Coefficients and ΔG_{inser}[a]

	partition coefficient ($\times 10^3$) and ΔG (kcal/mol)			
lipid	Pep33Ser	Pep33Ala	PepNH1	Pep62
PC	*b*	17.1 ± 1.7 (−5.6)	*b*	110 ± 33 (−6.7)
PC/OA (1/1)	15.4 ± 0.5 (−5.6)	29 ± 4 (−6.0)	95 ± 27 (−6.6)	194 ± 40 (−7.1)
PC/PG (1/1)	44 ± 4 (−6.2)	119 ± 20 (−6.8)	670 ± 50 (−7.8)	2690 ± 310 (−8.6)

[a] Peptide−vesicle binding was analyzed by a filtration assay, as described in Experimental Procedures. Partition coefficients were calculated from data obtained near the midpoints of the binding curves, in which >20 and <90% of the peptide was bound, except for Pep62 binding to PC/PG (>90% was bound even at the lowest lipid concentration). For Pep62, the ratio of peptide trapped on the filter/free peptide in the absence of lipid vesicles (0.2) was subtracted from the ratio of bound/free Pep62 obtained in the presence of the lipid vesicles. K_x values are the averages ± the SD of five to ten determinations. [b] No significant binding above background in 10 separate trials. The limit of sensitivity for the K_x value is $\sim 5 \times 10^3$ (~5 kcal/mol). The numbers in parentheses indicate the ΔG_{inser} ($=-RT \ln K_x$).

Figure 4 also shows the effects of PC and PG vesicles on the CD spectra of the peptides. The spectra of each peptide in the presence of PG vesicles were characteristic of α-helical structure (estimated ~50% helix, Table 2). PC/oleic acid (1/1) vesicles at a lipid/peptide ratio of 133 promoted the same helical content (Table 2). PC vesicles caused no change in the CD spectra of Pep33Ser or PepNH1 but significantly increased the helical character of the spectrum of Pep33Ala or Pep62 compared to that in buffer alone (Figure 4 and Table 2). There was a fairly good correspondence between the PC/peptide ratio resulting in increased helical content and increased physical binding of Pep33Ala or Pep62 (data not shown). Addition of PC/DAG did not significantly change the spectra of any peptide from that obtained in the presence of PC (Table 2). These results demonstrate a lipid-selective stabilization of an α-helical conformation for the entire domain M. The relative selectivities for anionic lipids demonstrated in the binding assay (Figure 3) were reflected in the conformational changes. Stringent selectivity for anionic lipids was observed for Pep33Ser and PepNH1, while Pep62 and Pep33Ala responded weakly to nonanionic and more strongly to anionic lipids.

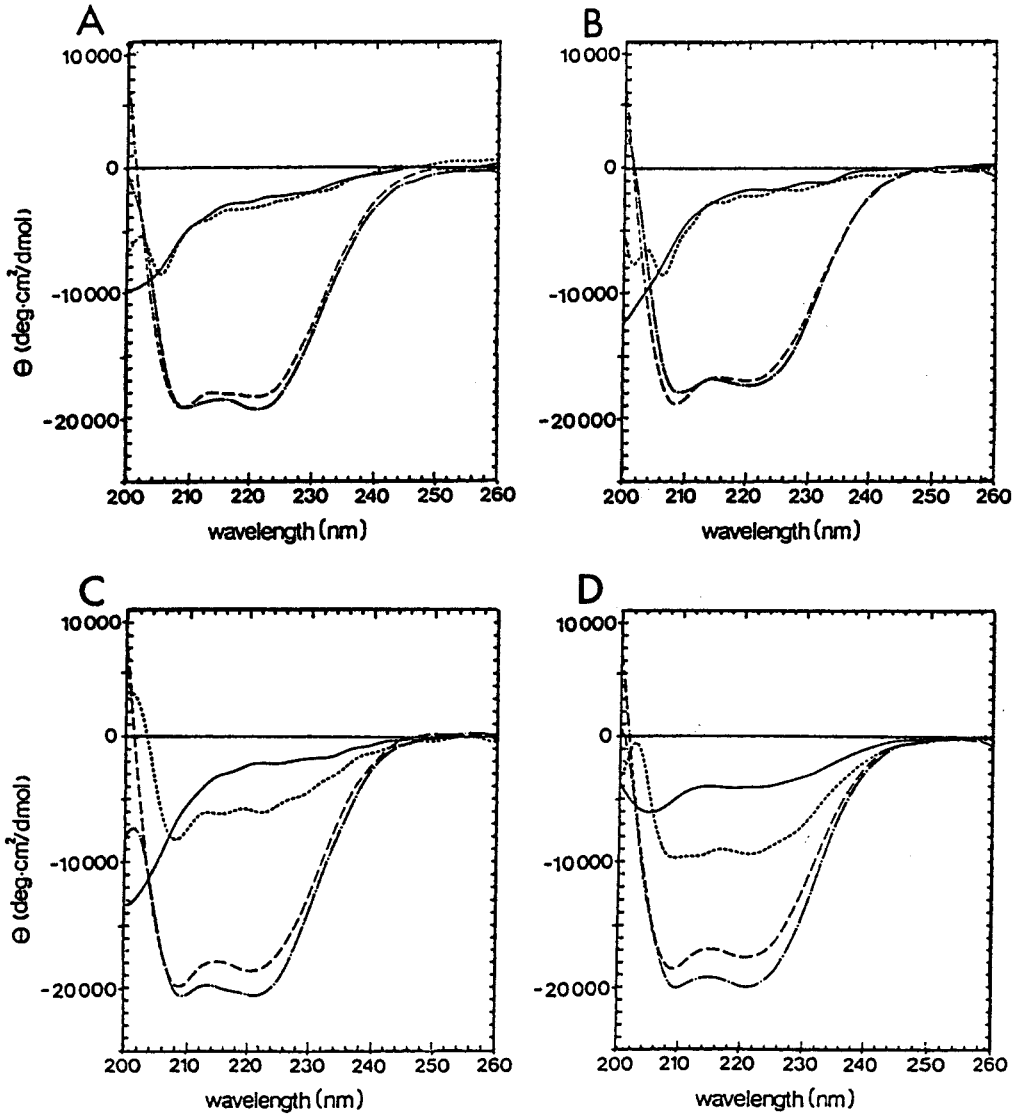

FIGURE 4: Circular dichroism spectra of the peptides. CD spectra of peptide (30 μM) in buffer (—), in a 50% trifluoroethanol solution (— —), and in the presence of PC vesicles (4 mM, ••) or PG vesicles (4 mM, —•—): (A) Pep33Ser, (B) PepNH1, (C) Pep33Ala, and (D) Pep62.

Table 2: Circular Dichroism Analysis of Peptides with Various Lipid Vesicles[a]

	$-[\Theta]_{222nm}$ (deg cm^2 dmol^{-1}) (estimated % helix)			
lipid	Pep33Ser	Pep33Ala	PepNH1	Pep62
none	2500 ± 300 (14%)	1940 ± 370 (13%)	1760 ± 20 (12%)	3540 ± 430 (13%)
PC	3100 ± 700 (16%)	5640 ± 380 (22%)	2100 ± 200 (13%)	9400 ± 940 (28%)
PC/DAG (3/1)	2300 ± 300 (14%)	7260 ± 1230 (26%)	2300 ± 500 (14%)	8560 ± 720 (26%)
PG	19 000 ± 1500 (56%)	17 800 ± 2300 (53%)	16 500 ± 800 (50%)	19 000 ± 1200 (52%)
PC/OA (1/1)	18 000 ± 2000 (53%)	23 000 ± 3500 (66%)	18 000 ± 2000 (53%)	18 000 ± 1000 (50%)
50% TFE[b]	18 200 ± 700 (54%)	17 500 ± 1000 (52%)	17 700 ± 900 (53%)	16 600 ± 2700 (46%)

[a] Samples contained 25 or 30 μM peptide and a 130-fold molar excess of lipid, except for Pep62 samples with PC or PC/DAG (lipid/peptide ratio was 50). [b] Samples contained TFE/TE buffer (1/1, v/v). Spectra were measured and % helix was estimated from $[\Theta]_{222}$ as described in Experimental Procedures. Data are average ± error of two to five independent experiments.

Fluorescence Studies Demonstrate Membrane Intercalation. To determine if the nonpolar face of the helical peptides intercalates into the hydrophobic membrane core, we monitored the fluorescence of a tryptophan residue positioned in the nonpolar face of each peptide helix (Figure 2). Addition of anionic vesicles composed of PG or PC/oleic acid increased the fluorescence intensity and shifted the emission maximum from 350 to 330 nm. These changes are indicative of a shift of the tryptophan from an aqueous to a nonpolar environment (*44*). The ratios of fluorescence intensity at

Table 3: Effect of Lipids on the Ratio of Peptide Fluorescence at 330 nm/350 nm[a]

lipid	fluorescence at 330 nm/350 nm			
	Pep33Ser	Pep33Ala	PepNH1	Pep62
none	0.62 ± 0.05	0.60 ± 0.05	0.59 ± 0.05	0.75 ± 0.02
PC	0.68 ± 0.03	0.83 ± 0.09	0.61 ± 0.02	0.89 ± 0.13
PC/DAG (3/1)	0.69 ± 0.03	0.84 ± 0.13	0.61 ± 0.02	0.99 ± 0.10
PC/PG (1/1)	1.14 ± 0.07	1.19 ± 0.05	1.04 ± 0.02	1.41 ± 0.04
PC/OA (1/1)	1.07 ± 0.01	1.21 ± 0.02	1.01 ± 0.03	ND

[a] The peptide concentration was 3.25 μM. Lipid concentrations were 0.5 mM, except for samples with Pep62 (0.162 mM). Fluorescence emission spectra were measured as described in Experimental Procedures. For representative spectra of Pep33Ser, see ref *10*. Data are the average ± error of two to twelve independent experiments.

Table 4: Quenching of Peptide Fluorescence by Aqueous Iodide[a]

lipid	% fluorescence quenching		
	Pep33Ser	Pep33Ala	PepNH1
none	48 ± 4	55 ± 2	58 ± 1
PC/diacylglycerol (3/1)	47 ± 6	38 ± 3	60 ± 3
PG	15 ± 2	11 ± 1	12 ± 4

[a] Peptide concentrations were 3.25 μM. Lipid vesicle concentrations were 0.5 mM. Spectra were measured as described in Experimental Procedures. % quench = $100(1 - F/F_o)$, where F is the fluorescence intensity of the quenched sample obtained in the presence of 0.2 M iodide and F_o is the fluorescence intensity of the unquenched sample with 0.2 M chloride in place of iodide. Data are the average ± error of two to four independent experiments.

330 nm/350 nm are reported in Table 3. Nonanionic lipids, such as PC or PC/DAG, caused no change in the F_{330}/F_{350} ratio of Pep33Ser or PepNH1 but did cause a significant increase in the F_{330}/F_{350} ratio of Pep33Ala and Pep62 (Table 3). Thus, Pep33Ala and Pep62 appeared to respond to nonanionic lipids to a much greater extent than Pep33Ser or PepNH1, consistent with the binding and CD analysis. The effects of PC/DAG vesicles on the fluorescence of Pep33Ala and Pep62 were not significantly different from the effects of PC alone.

The influence of lipids on the penetration of the peptides was also monitored by testing the accessibility of the tryptophan to the aqueous phase quencher, iodide (*44*, *45*). Burial of the Trp in a membrane would reduce the quenching efficiency of iodide. In the absence of lipid vesicles, the fluorescence of each peptide at 350 nm was quenched 50−60% by 0.2 M NaI (Table 4). In the presence of PG, the fluorescence quenching by iodide was reduced to 11−15%, suggesting shielding by the PG vesicles. A decrease in the iodide quenching was also observed in the presence of a 300-fold molar excess of PC/oleic acid vesicles (data not shown). Iodide quenching of Pep33Ser and PepNH1 in the presence of nonanionic vesicles was the same as that obtained in the absence of lipid (Table 4). However, iodide quenching of Pep33Ala was reduced in the presence of PC/DAG vesicles, suggesting partial shielding of the tryptophan by these nonanionic vesicles.

To further probe the membrane localization of the peptide tryptophan, we utilized a quencher that is covalently linked to the *sn*-2 acyl chain of a lipid, 9,10-dibromo-PC (Br-PC). Quenching of the tryptophan fluorescence would occur only if the residue were intercalated into the hydrophobic core of the bilayer. Table 5 shows the quenching of the four peptides

Table 5: Quenching of Peptide Fluorescence by 9,10-Dibromo-PC[a]

lipid	% fluorescence quenching by Br-PC			
	Pep33Ser	Pep33Ala	PepNH1	Pep62
PC	4 ± 1	27 ± 6[b]	0 ± 4	23 ± 1
PC/DAG (3/1)	8 ± 2	38 ± 8[b]	6 ± 3	49 ± 9
PG/PG (1/1)	57 ± 2	61 ± 5	56 ± 1	62 ± 1

[a] Peptide concentrations were 3.25 μM. Lipid concentrations were 0.5 mM, except for samples with Pep62 (0.162 mM). The peptides were added to vesicles composed of the indicated lipid. In unquenched samples, the PC was egg PC; in quenched samples, 50% of the total lipid was 9,10-dibromo-PC, and the balance of the PC was egg PC. % quench = $100(1 - F/F_o)$, where F is the fluorescence intensity of the quenched sample containing 9,10-dibromo-PC and F_o is the fluorescence intensity of the unquenched sample containing egg PC. Data are the average ± error of two to seven independent experiments. [b] $P = 0.08$ in an unpaired T test.

by lipid vesicles containing 50% Br-PC. The fluorescence was quenched ~60% by PC/PG (1/1) vesicles. When incorporated into PC vesicles, Br-PC caused only ≤4% quenching of PepNH1 or Pep33Ser fluorescence, suggesting no peptide intercalation into these vesicles. PC/DAG vesicles containing the probe were also ineffective quenchers of these peptides (Table 5). The fluorescence of Pep33Ala or Pep62, on the other hand, was quenched ~25% by PC vesicles containing Br-PC and 36 or 49%, respectively, by PC/DAG vesicles. This data is consistent with all the previous observations suggesting that Pep33Ala and Pep62 show less stringent selectivity for anionic membranes than do Pep33Ser or PepNH1.

This analysis suggested a significant effect of DAG on the membrane interaction of Pep33Ala and Pep62, in contrast to the CD data (Table 2) and fluorescence blue shifts (Table 3), which indicated no differences between the effects of PC and PC/DAG. One possible explanation could be that the dibromo adduct on the acyl chain is not a silent probe, and that it has a selective effect on the PC/DAG bilayer. To test this idea, we measured the CD spectra of Pep33Ala in the presence of PC or PC/DAG (3/1) vesicles with or without 50 mol % Br-PC. The $[\Theta]_{222\ nm}$ (percent helix) values were as follows: PC, −5950 (23%); PC/DAG (3/1), −7601 (27%); Br-PC/PC (1/1), −11 233 (36%); and Br-PC/PC/DAG (2/1/1), −12 900 (40%). This analysis suggested that the bromo adduct enhances the helix stabilization by both PC and PC/DAG vesicles.

Surface Activity of the CT Peptides. The tendency of Pep33Ser, Pep33Ala, and Pep62 to orient at the air−water interface in the absence of a spread lipid monolayer was examined by measuring surface pressure increases as a function of peptide concentration in the subphase. The surface pressure increased in a sigmoidal fashion for each peptide and reached a plateau at ~0.2 μM peptide. Pep62 was the most effective modulator of the surface pressure, followed by Pep33Ala, followed by Pep33Ser (Figure 5). The saturation pressures were 12, 22, and 26 dyn/cm for Pep33Ser, Pep33Ala, and Pep62, respectively. These data suggest that the domain M peptides have strong intrinsic surface activity, which ranks in the order of the hydrophobicity of their nonpolar helical faces.

The surface pressure was monitored upon addition of 0.1−0.45 μM peptide to the subphase beneath monolayers of PC, sphingomyelin (SM), PS, PG, or cardiolipin spread at 5 dyn/

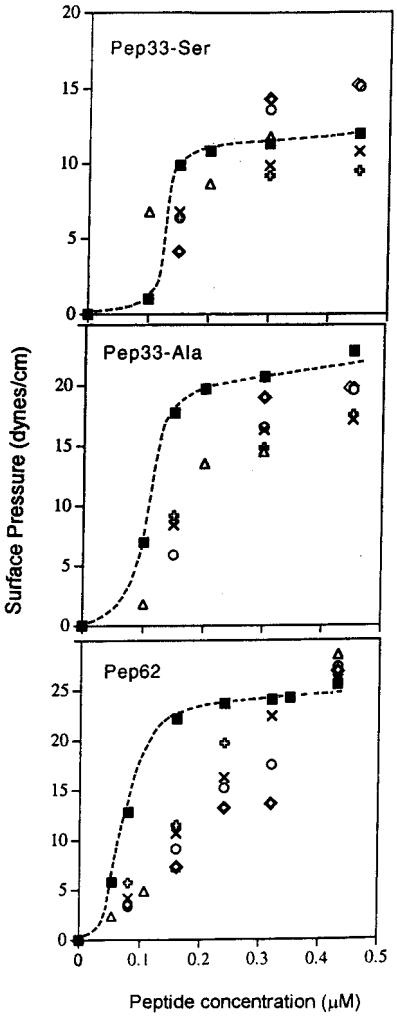

FIGURE 5: Effects of peptides on the surface pressure. The surface pressure was measured after equilibration with peptide as described in Experimental Procedures, in the absence (■) or presence of lipid monolayers spread at 5 dyn/cm: (×) PC, (✣) sphingomyelin, (△) PS, (◇) cardiolipin, and (○) PG.

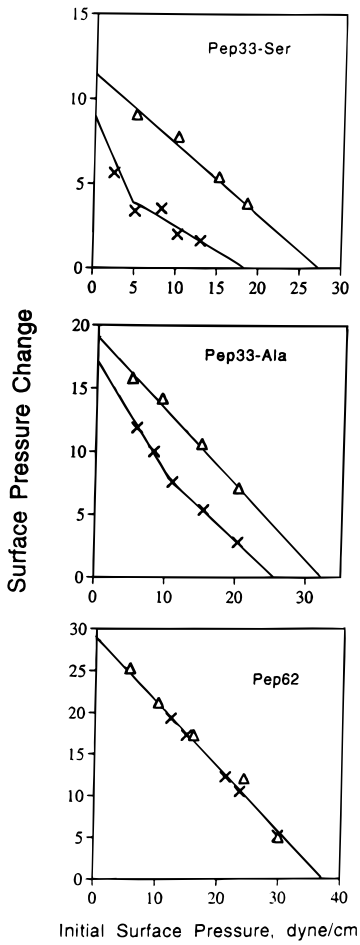

FIGURE 6: Effect of initial surface pressure on peptide-induced changes in monolayer surface pressures. The peptide concentration in the subphase was 0.5 μM: PS monolayer (△) and PC monolayer (×).

cm. In general, the effect of the lipid monolayers was to reduce the surface pressure increase due to peptide (Figure 5). This unanticipated effect was especially apparent for Pep33Ala, and Pep62 at subsaturating peptide concentrations (<0.3 μM), and was observed with both zwitterionic and anionic lipids. A surface pressure above that obtained with peptide alone was only obtained in the case of Pep33Ser (≥0.3 μM) added to PG or cardiolipin monolayers. These data suggested two possibilities: (1) that lipid and peptide might compete for positions at the interface, rather than interact with each other, or (2) that peptide−lipid interaction leads to condensation of lipids and/or peptide in the monolayer.

The set of experiments shown in Figure 5 utilized a surface pressure of 5 dyn/cm, corresponding to a very low packing density of lipids compared to that of phospholipids in a bilayer vesicle. In another set of experiments, the peptide-dependent surface pressure change ($\Delta\pi$) was studied as a function of the initial monolayer surface pressure (π_i). $\Delta\pi$ values were greatest at all π_i for Pep62, followed by those for Pep33Ala, and those for Pep33Ser (Figure 6). The $\Delta\pi$ versus π_i plots for Pep62 with monolayers of PC or PS were identical, suggesting no lipid selectivity for Pep62 with monolayer pressures ≤30 dyn/cm. The slope of either plot was −0.77 (Figure 6, bottom panel). If peptide and lipid do not interact, but merely compete with each other on the surface, the slope of this plot will be −1. For the 33mer peptides, significant differences were obtained for PC and PS monolayers. For PS monolayers, the plots of $\Delta\pi$ versus π_i were linear with slopes of −0.40 and −0.58 for Pep33Ser and Pep33Ala, respectively, whereas the plots for PC monolayers were two-component plots. The slopes were nearly −1 when $\pi_i = 5$ (Pep33Ser) or 10 dyn/cm (Pep33Ala), suggesting that PC and peptide do not interact, but merely compete with each other for a position at the air−water interface. Above 5 dyn/cm, slopes were more than −1 (−0.25 for Pep33Ser and −0.51 for Pep33Ala). This analysis provided evidence for interactions between anionic lipids and all peptides at all π_i values. Interactions between PC and Pep62 were indicated at all π_i values, while interactions between PC and the 33mer peptides were suggested only at higher π_i values.

The interaction of the domain M peptides with the phospholipids would involve an intercalation between the molecules of the monolayer. The critical exclusion surface pressure above which there can be no peptide penetration is obtained from the *x*-intercept of the plots in Figure 6. This critical pressure decreased in the order Pep62 > Pep33Ala > Pep33Ser. Thus, the longer, more hydrophobic Pep62 can insert into monolayers that are more compressed than those

that accommodate insertion of the 33mer peptides. For Pep62, the critical pressure π_c for insertion into PC or PS monolayers was 37 dyn/cm. For Pep33Ala, the π_c for insertion into a PS or PC monolayer was 33 or 26 dyn/cm, respectively. For Pep33Ser, the π_c for insertion into a PS or PC monolayer was 28 or 19 dyn/cm, respectively.

DISCUSSION

All Peptides Derived from Domain M Interact Selectively with Anionic Membranes, in an α-Helical Conformation. The peptide derived from the N-terminal half of domain M, PepNH1, the C-terminal derived Pep33Ser, and a 62mer peptide which spans the entire domain M intercalated into membranes with selectivity for anionic lipids, which stabilized an α-helical conformation. In a separate study, intercalation of the 62mer peptide in PC/oleic acid membranes was demonstrated by its labeling with the hydrophobic photoreactive probe [^{125}I]TID (*30*). Thus, a role for the entire domain M in membrane interaction is suggested.

In a recent mutagenesis study, the region corresponding to the second 11mer repeat in domain M (residues 266−277) appeared to be necessary for binding of GST−CT fusion proteins to PC/oleic acid vesicles (*46*). Fusion proteins containing the first or third 11mer repeat, but lacking the second, did not bind to the vesicles, while a fusion protein containing only the second repeat did bind. This observation might contradict our conclusion based on the peptide work that domain M in its entirety interacts as a structural unit with membranes. However, the structures of the GST−CT mutant proteins were not analyzed. It is possible that all the fusion proteins disrupted the α-helicity of the domain M fragments, except for the constructs containing residues 267−277. This possibility is supported by secondary structure algorithms which indicate that the second 11mer repeat (residues 267−277) has the highest potential for α-helical conformation.

Domain M Is Necessary but Not Sufficient for the Interaction with Membranes Containing DAG. Many studies suggest that CT translocation to cell membranes and CT activation in vitro can be stimulated by DAG (*5*, *8*, *47*−*49*). Removal of domain M by chymotrypsin degradation (*11*) or cDNA mutation (*18*) produced fragments that were unable to bind to vesicles containing DAG, suggesting that this domain is required for binding. Furthermore, hydrophobic photolabeling of CT in the presence of PC/DAG vesicles indicated that domain M is the predominant intercalated region of the protein (*30*). However, none of the domain M-derived peptides, including Pep62, showed any specificity for PC/DAG vesicles over PC alone, on the basis of CD spectra and fluorescence blue shifts. Br-PC quenching, on the other hand, did suggest a selective effect of DAG on the membrane intercalation of Pep33Ala and Pep62. CD analysis indicated that inclusion of 50% Br-PC within PC or PC/DAG vesicles promoted an approximately equal stabilization of the membrane-associated α-helical conformation. It is likely that the bromines, although positioned at the 9,10-carbon on the *sn*-2 chain, populate the interfacial region of the bilayer more so than the underivatized hydrocarbon chain. The surfacing of the brominated chain might be facilitated by bilayers containing DAG, since its very small headgroup would better accommodate the increased interfacial volume. Thus, the enhanced quenching by Br-PC in a PC/DAG bilayer might reflect an effect on the orientation of the quenching group rather than an effect on peptide intercalation. This idea is supported by the equal effects of Br-PC and Br-PC/DAG on helix stabilization. We conclude that, although domain M is required for the binding of CT to DAG-containing membranes, it is not sufficient. Perhaps another site cooperates with domain M in the interaction with membranes containing DAG.

Role of Peptide Charge and Hydrophobicity in the Determination of Lipid Selectivity. All peptides analyzed had higher affinity for anionic than for zwitterionic lipids, suggesting an electrostatic component to the binding. Recently solved NMR structures of two domain M peptides reveal that the majority of the basic side chains are positioned along the polar and/or nonpolar interfaces over the entire length of the amphipathic helix, while the acidic side chains are mostly segregated to the center of the polar face (*21*; see also Figure 2). This explains why even Pep33Ser and Pep33Ala (with net charges of −2) have preference for anionic lipids.

The selectivity for anionic lipids was the greatest for the peptide with a net charge of +3, PepNH1. The N-terminal half of domain M houses the highest concentration of Lys and Arg side chains, but the least hydrophobic residues (see Figure 2). The N-terminal peptide had a higher affinity for anionic lipids than the C-terminal peptide, Pep33Ser. Pep33Ser has the more hydrophobic face of the two. Thus, the increased number of interfacial lysines must dictate the ∼15-fold increase in K_x for PC/PG vesicles of PepNH1 versus that for Pep33Ser. In general, the lower the hydrophobicity of the CT peptide, the greater the selectivity for anionic phospholipids, i.e., the greater the role for electrostatics in binding.

Pep62 had the highest affinity of all peptides for both anionic and nonanionic lipids. This may reflect both a larger hydrophobic interaction, due to the longer hydrophobic face (calculated $\Delta G_H = -53$ kcal/mol; *50*), and a larger number of charged residues involved in electrostatic interactions. Since the difference in K_x for PC versus PC/PG was only ∼30-fold, the principal component of the binding interaction is the hydrophobic effect (−6.7 kcal/mol). Electrostatic interactions contribute only an additional 2 kcal/mol to the free energy of binding (Table 1).

The role of the serines which interrupt the nonpolar face was probed by substitution with alanine. The Ser → Ala replacement increased the peptide's membrane affinity and decreased its stringent anionic lipid specificity. Pep33Ser did not completely bind to the anionic lipids over the lipid/peptide range tested, and its binding to nonanionic vesicles could not be detected. Pep33Ala had an increased affinity for anionic lipids and also interacted with PC, as detected by the direct binding assay, CD, fluorescence, and monolayer pressure changes. Thus, these three serine residues in CT may function to attenuate the membrane affinity of the amphipathic helix and, in so doing, enhance lipid selectivity. Liu and Deber (*51*) have also observed that marginally hydrophobic model peptides are more dependent on anionic lipids and electrostatic attraction for membrane association than their more hydrophobic analogues.

Domain M Binds with Its Helix Axis Parallel to the Lipid Surface. NMR data suggest an unbent α-helix for domain

M when it is bound to SDS micelles (*21*). Both N- and C-terminal regions flanking domain M extend into the same aqueous compartment (*11*). It is thus difficult to conceive of a membrane orientation for domain M other than one with the helix axis parallel to the surface. The strong surface-seeking tendencies of the CT peptides [which exceed that of, e.g., surfactin, a strong surfactant peptide from *Bacillus subtilis* (*52*)] are a further argument for such an orientation. It also supports the dominance of the hydrophobic effect in the binding of the CT peptides to interfaces. The surface activity of the three CT peptides tested was directly related to the hydrophobicity of their nonpolar helical faces and not to their helical hydrophobic moment (see Figures 1 and 5).

Lipid−Peptide Complex Formation. If peptide and lipid molecules mix ideally at the interface, the pressure increase resulting from the mixture should equal the sum of their individual pressures (*53*). However, the surface pressures due to lipid and peptide were less than additive, suggestive of complex formation (*53*). For example, the surface pressure induced by 0.2 μM peptide was reduced by the spread lipid monolayer (Figure 5). This effect was especially apparent for Pep62. Peptide binding could neutralize the negative charge on the lipid headgroups, leading to condensation of lipids in the monolayer. Moreover, the phospholipid surface may have promoted the folding of the peptides from random coil to a more compact α-helix, contributing to the surface pressure reduction. CD evidence showing that anionic lipids promote helix formation in all the peptides supports this notion. We envision that the peptides initially bind in an extended conformation at the air−water interface at low lipid packing densities. Encounters between lipid and peptide induce aggregation of the lipid molecules into a lipid−peptide complex which concomitantly triggers folding into an α-helix. This process reduces the surface area per molecule in the monolayer.

Lipid Packing Density Influences the Lipid Selectivity for Binding of Domain M Peptides. One component of anionic phospholipids that may facilitate CT binding is the charge repulsion at the surface which leads to looser packing, i.e., greater surface area per molecule (*54*). The packing density of zwitterionic lipids in bilayers may present too great a barrier for domain M intercalation. If the mechanism whereby anionic lipids promote the intercalation of CT peptides is via decreasing the packing density, then the peptides might also bind to zwitterionic monolayers at low packing densities. Packing density in monolayer films can be varied by controlling the initial surface pressures. We observed for the three peptides tested (Figures 5 and 6) a relaxation of the preference for anionic lipids at π_i values below or near the bilayer equivalence value of 31 dyn/cm (*55*−*57*). Pep62 interacted equally with PS and PC monolayers at π_i values below 30 dyn/cm, whereas all the data using vesicles had supported a selectivity for anionic lipids. Whereas binding of Pep33Ser to PC vesicles could not be detected, an interaction with the PC monolayer was observed at π_i values (and PC surface densities) sufficient to foster hydrophobic associations between lipid and peptide. The selectivity for anionic versus zwitterionic lipids increased in the order Pep62 < Pep33Ala < Pep33Ser, in accordance with the vesicle binding analyses. The preference of the 33mer peptides for PS over PC could be explained by the greater area per molecule of the PS versus PC at the same pressure, which would better accommodate these less surface-active peptides. Together, these data indicate that selectivity for anionic lipids is weakened by low lateral packing pressure. This supports the proposal that lipid packing density is a barrier against the membrane binding of CT, which can be alleviated by the looser packing of anionic lipids.

ACKNOWLEDGMENT

We thank Ian Clark-Lewis and Philip Owen for peptide synthesis.

REFERENCES

1. Houweling, M., Jamil, H., Hatch, G., and Vance, D. E. (1994) *J. Biol. Chem. 269*, 7544−7551.
2. Wang, Y., and Kent, C. (1995) *J. Biol. Chem. 270*, 17843−17849.
3. Arnold, R. S., DePaoli-Roach, A., and Cornell, R. B. (1997) *Biochemistry 36*, 6149−6156.
4. Feldman, D. A., and Weinhold, P. A. (1987) *J. Biol. Chem. 262*, 9075−9081.
5. Johnson, J. E., Kalmar, G. B., Sohal, P., Walkey, C., Yamashita, S., and Cornell, R. B. (1992) *Biochem. J. 285*, 815−820.
6. Cornell, R., and Vance, D. E. (1987) *Biochim. Biophys. Acta 919*, 37−48.
7. Cornell, R. B. (1991) *Biochemistry 30*, 5873−5880.
8. Cornell, R. B. (1991) *Biochemistry 30*, 5881−5888.
9. Arnold, R. S., and Cornell, R. B. (1996) *Biochemistry 35*, 9917−9924.
10. Johnson, J. E., and Cornell, R. B. (1994) *Biochemistry 33*, 4327−4335.
11. Craig, L., Johnson, J. E., and Cornell, R. B. (1994) *J. Biol. Chem. 269*, 3311−3317.
12. Tsukagoshi, Y., Nikawa, J., and Yamashita, S. (1987) *Eur. J. Biochem. 169*, 477−486.
13. Park, Y. S., Sweitzer, T. D., Dixon, J. E., and Kent, C. (1993) *J. Biol. Chem. 268*, 16648−16654.
14. Bork, P., Holm, L., Koonin, E., and Sander, C. (1995) *Proteins: Struct., Funct., Genet. 22*, 259−266.
15. Veitch, D. P., and Cornell, R. B. (1996) *Biochemistry 35*, 10743−10750.
16. Wang, Y., and Kent, C. (1995) *J. Biol. Chem. 270*, 18948−18952.
17. MacDonald, J. I. S., and Kent, C. (1994) *J. Biol. Chem. 269*, 10529−10537.
18. Cornell, R. B., Kalmar, G. B., Kay, R. J., Johnson, M. A., Sanghera, J. S., and Pelech, S. P. (1995) *Biochem. J. 310*, 699−708.
19. Yang, W., and Jackowski, S. (1995) *J. Biol. Chem. 270*, 16503−16506.
20. Wang, Y., MacDonald, J., and Kent, C. (1993) *J. Biol. Chem. 268*, 5512−5518.
21. Dunne, S. J., Cornell, R. B., Johnson, J. E., Glover, N. R., and Tracey, A. S. (1996) *Biochemistry 35*, 11975−11984.
22. Segrest, J. P., Garber, D. W., Brouillette, C. G., Harvey, S. C., and Anantharamaiah, G. M. (1994) *Adv. Protein Chem. 45*, 303−369.
23. Rozek, A., Buchko, G. W., and Cushley, R. J. (1995) *Biochemistry 34*, 7401−7408.
24. Wang, G., Sparrow, J. T., and Cushley, R. J. (1997) *Biochemistry 36*, 13657−13666.
25. Picot, D., Loll, P., and Garavito, R. M. (1994) *Nature 367*, 243−249.
26. Gilbert, G. E., and Baleja, J. D. (1995) *Biochemistry 34*, 3022−3031.
27. Huang, A. H. C. (1994) *Curr. Opin. Struct. Biol. 4*, 493−498.
28. Epand, R. M., Shai, Y., Segrest, J. P., and Anantharamaiah, G. M. (1995) *Biopolymers 37*, 319−338.

29. Antonny, B., Beraud-Dufour, S., Chardin, P., and Chabre, M. (1997) *Biochemistry 36*, 4675−4684.
30. Johnson, J. E., Aebersold, R., Drobnies, A., and Cornell, R. B. (1997) *Biochim. Biophys. Acta 1324*, 273−284.
31. Myher, J., and Kuksis, A. (1979) *Can. J. Biochem. 57*, 117−124.
32. Bartlett, G. R. (1959) *J. Biol. Chem. 234*, 466−468.
33. Kalmar, G. B., Kay, R., Lachance, A., Aebersold, R., and Cornell, R. B. (1990) *Proc. Natl. Acad. Sci.* U.S.A. *87*, 6029−6033.
34. Clark-Lewis, I., Moser, B., Walz, A., Baggiolini, M., Scott, G. J., and Aebersold, R. (1991) *Biochemistry 30*, 3128−3135.
35. Tamm, L. (1994) in *Membrane Protein Structure* (White, S. H., Ed.) pp 283−313, Oxford Press, Oxford, U.K.
36. Roth, M. (1971) *Anal. Chem. 43*, 880−882.
37. Chen, Y.-H., Yang, J. T., and Chau, K. H. (1974) *Biochemistry 13*, 3350−3359.
38. Chang, C. T., Wu, C.-S. C., and Yang, J. T. (1978) *Anal. Biochem. 91*, 13−31.
39. Sonnichsen, F. D., Van Eyk, J. E., Hodges, R. S., and Sykes, B. D. (1992) *Biochemistry 31*, 8790−8798.
40. Yu, H., and Hui, S.-W. (1992) *Biochim. Biophys. Acta 1107*, 245−254.
41. Killian, J. A., Keller, R., Struyve, M., DeKroon, A., Tommassen, J., and de Kruijff, B. (1990) *Biochemistry 29*, 8131−8137.
42. McKnight, C. J., Rafalski, M., and Gierasch, L. M. (1991) *Biochemistry 30*, 6241−6246.
43. Tang, W., Keesler, G. A., and Tabas, I. (1997) *J. Biol. Chem. 272*, 13146−13151.
44. Lakowicz, J. R. (1983) *Principles of Fluorescence Spectroscopy*, Plenum Press, New York.
45. Eftink, M. R. (1991) in *Biophysical and Biochemical Aspects of Fluorescence Spectroscopy* (Dewey, T. G., Ed.) Plenum Press, New York.
46. Yang, J., Wang, J., Tseu, I., Kuliszewski, M., Lee, W., and Post, M. (1997) *Biochem. J. 325*, 29−38.
47. Slack, B. E., Breu, J., and Wurtman, R. J. (1991) *J. Biol. Chem. 266*, 24503−24508.
48. Utal, A. K., Jamil, H., and Vance, D. E. (1991) *J. Biol. Chem. 266*, 24084−24091.
49. Tronchere, H., Planat, V., Record, M., Terce, F., Ribbes, G., and Chaps, H. (1995) *J. Biol. Chem. 270*, 13138−13146.
50. Engleman, D. M., Steitz, T. A., and Goldman, A. (1986) *Annu. Rev. Biophys. Chem. 15*, 321−353.
51. Liu, L.-P., and Deber, C. M. (1997) *Biochemistry 36*, 5476−5482.
52. Maget-Dana, R., and Ptak, M. (1995) *Biophys. J. 68*, 1937−1943.
53. Jones, M., and Chapman, D. (1995) *Micelles, Monolayers, and Biomembranes*, pp 24−63, Wiley-Liss, New York.
54. Ohki, S., and Duzgunes, M. (1979) *Biochim. Biophys. Acta 552*, 438−449.
55. Blume, A. (1979) *Biochim. Biophys. Acta 577*, 32−38.
56. Demel, R. A., VanKessel, W., Zwaal, R., Roelfsen, B., and VanDeenen, L. L. (1975) *Biochim. Biophys. Acta 406*, 97−101.
57. Portlock, S., Lee, Y., Tomich, J., and Tamm, L. (1992) *J. Biol. Chem. 267*, 11017−11022.
58. Eisenberg, D., Weiss, R., and Terwilliger, T. (1984) *Proc. Natl. Acad. Sci. U.S.A. 81*, 140−144.
59. Finer-Moore, J., and Stroud, R. (1984) *Proc. Natl. Acad. Sci. U.S.A. 81*, 155−159.

BI980340L